



## Application of $\beta$ -NMR to spectroscopy and imaging

Yutaka Mizoi<sup>1,9,\*</sup>, Mototsugu Mihara<sup>2,9</sup>, Yoko Kimura<sup>2,9</sup>, Takato Sugisaki<sup>2,9</sup>, Gen Takayama<sup>2</sup>, Masaomi Tanaka<sup>3,9</sup>, Daiki Nishimura<sup>4</sup>, Yurika Otani<sup>2,9</sup>, Miki Fukutome<sup>2</sup>, Ryo Taguchi<sup>2</sup>, Chen Sitan<sup>2</sup>, Soshi Ishitani<sup>2</sup>, Rina Miyahara<sup>2</sup>, Kaoru Watanabe<sup>2</sup>, Mitsunori Fukuda<sup>2</sup>, Takuji Izumikawa<sup>5</sup>, Norihide Noguchi<sup>5</sup>, Kazuya Takatsu<sup>5</sup>, Hiroyuki Takahashi<sup>4</sup>, Asahi Yano<sup>6</sup>, Hibiki Seki<sup>7,9</sup>, Takashi Ohtsubo<sup>8</sup>, Kensaku Matsuta<sup>2</sup>, Atsushi Kitagawa<sup>8</sup>, Shinji Sato<sup>8</sup>

<sup>1</sup>Osaka Electro-Communication University (OECU), 18-8 Hatsucho Neyagawa, Osaka, 572-8530, Japan,

<sup>2</sup>Osaka University, 1-1 Machikaneyama Toyonaka, Osaka, 560-0043, Japan,

<sup>3</sup>RIKEN, 2-1 Hirosawa Wako, Saitama, 351-0198, Japan,

<sup>4</sup>Tokyo City University, 1-28-1 Tamazutsumi Setagaya, Tokyo, 158-8557, Japan,

<sup>5</sup>Niigata University, 8050 Ikarashi 2-no-cho Nishi-ku, Niigata, 950-2181, Japan,

<sup>6</sup>University of Tsukuba, 1-1-1 Tennodai Tsukuba, Ibaraki, 305-8577, Japan,

<sup>7</sup>Saitama University, 255 Shimo-Okubo Sakura-ku Saitama, Saitama, 338-8570, Japan,

<sup>8</sup>National Institute for Quantum and Radiological Science and Technology (QST),

4-9-1 Anagawa Inage-ku Chiba, Chiba, 263-8555, Japan,

<sup>9</sup>Open-It, <https://openit.kek.jp>

\*E-mail: [mizoi@osakac.ac.jp](mailto:mizoi@osakac.ac.jp)

**Abstract:** Nuclear magnetic resonance (NMR) using  $\beta$ -decay radioisotopes, known as “ $\beta$ -NMR,” is used for research in nuclear physics. Recently, nuclear magnetic moments of  $\beta$ -decay radioisotopes have been precisely measured by  $\beta$ -NMR. Therefore,  $\beta$ -decay radioisotopes can be used for NMR spectroscopy in material sciences. Nuclei, whose spin is zero, such as  $^{12}\text{C}$  and  $^{16}\text{O}$ , cannot be used in conventional NMR. However, nonzero-spin radioactive isotopes of carbon and oxygen can be used in  $\beta$ -NMR. This advantage is powerful for investigating organic materials that cannot be investigated using conventional NMR. A technique is being developed to extend  $\beta$ -NMR for imaging use in magnetic resonance imaging (MRI). In this study, the imaging function was realized by installing  $\beta$ -ray tracking detectors in a  $\beta$ -NMR device. Nuclear-spin-polarized radioisotopes were injected into a sample, and  $\beta$ -rays were emitted from their positions. Consequently, one could track back  $\beta$ -ray source positions on the sample. These detectors were installed into a dipole magnet to observe the magnetic resonances. A radio frequency coil was installed surrounding the sample. By combining information about the  $\beta$ -ray tracks and magnetic resonances, it was possible to obtain NMR spectra and images. This method is called “ $\beta$ -MRI.” The system was evaluated, and its performances were estimated.

**Keywords:** Nuclear magnetic resonance (NMR), Magnetic resonance imaging (MRI),  $\beta$ -decay radioisotope,  $\beta$ -ray detector.

### I. INTRODUCTION

Since nuclear magnetic resonance (NMR) was developed by Rabi [1,2], NMR spectroscopy has been put to practical use in

many fields of science and engineering. NMR cannot be observed using nuclei with spins of zero. Thus, observing the NMR of such elements as  $^{12}\text{C}$  and  $^{16}\text{O}$  is difficult. Short-lived  $\beta$ -decay radioisotopes (RIs) exhibit the

well-known asymmetry of  $\beta$ -ray spatial distribution. Utilizing this asymmetry, one can perform NMR spectroscopy using RIs [3,4]. This technique is called “ $\beta$ -NMR.” Because oxygen and carbon RIs have nonzero spin, they can be used to perform  $\beta$ -NMR spectroscopy. Atoms with numbers of Avogadro-constant order are necessary for observing the NMR spectrum. However, the required minimum number of RI atoms is  $10^7$  for a  $\beta$ -NMR spectrograph. This high sensitivity of  $\beta$ -NMR is useful for various types of research.

Magnetic resonance imaging (MRI) is one of application of NMR [5,6]. MRI is a powerful tool in medical fields, but the MRI currently in practical use only employs hydrogen. Thus, a new MRI method utilizing  $\beta$ -NMR, called “ $\beta$ -MRI,” was developed. MRI utilizes changes in resonance frequency in the magnetic-field gradient for obtaining images. However,  $\beta$ -MRI utilizes  $\beta$ -ray tracks for imaging. Previously,  $\beta$ -ray tracking detectors were developed and installed in a  $\beta$ -NMR instrument [7]. For evaluating the present  $\beta$ -MRI system, a sample was irradiated by nuclear-spin-polarized  $^{12}\text{B}$  beams. The sample shape was obtained with millimeter-order resolution. Computer simulation was used to find ways to improve the image resolution.

## II. EXPERIMENTAL SETUP AND PROCEDURE

### A. Production of nuclear-spin-polarized RI beam

For the  $\beta$ -NMR measurement, spin-polarized RI nuclei are necessary. A projectile-fragmentation reaction was employed to produce the polarized  $^{12}\text{B}$  beams [8]. Experiments were performed at a secondary-beam course of a

heavy-ion synchrotron facility, HIMAC, National Institute for Quantum Science and Technology (QST), Japan [9,10]. The  $^{12}\text{B}$  beam was produced by bombarding a  $^{13}\text{C}$  beam with an energy of 70 MeV/nucleon on a  $^9\text{Be}$  target. Injecting a  $^{13}\text{C}$  beam with an angle of  $2^\circ$  with respect to the beam axis makes it possible to select nuclear-spin-polarized  $^{12}\text{B}$  beams. The 20%-polarized  $^{12}\text{B}$  beams were obtained with an energy of 45 MeV/nucleon and an intensity of 200 particles per second.

### B. Setup of $\beta$ -MRI system and experiment

As shown in Fig.1, the  $\beta$ -NMR instrument consists of a dipole magnet, a radio frequency (RF) radiator coil, and  $\beta$ -ray detectors. A sample is placed inside the RF radiator coil. The polarized RI ions are implanted into the sample.  $^{12}\text{B}$  undergoes  $\beta$ -decay with a half-life of 20 ms. The  $\beta$ -ray spatial distribution is described by  $W(\theta) \sim 1 + A P \cos \theta$ . Here,  $\theta$  is an angle of  $\beta$ -ray emission with respect to the magnetic-field axis, and  $A$  is an asymmetry parameter that depends on nuclear species. For  $^{12}\text{B}$ ,  $A = -1$ . By counting  $\beta$ -rays using upside and downside counters,  $W(0^\circ)$  and  $W(180^\circ)$  can be determined. By calculating their ratio,  $W(0^\circ)/W(180^\circ)$ , one can determine the nuclear-spin polarization,  $P$ . The polarization can be controlled by an

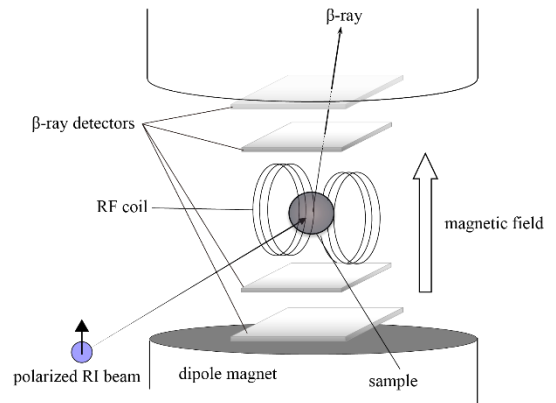
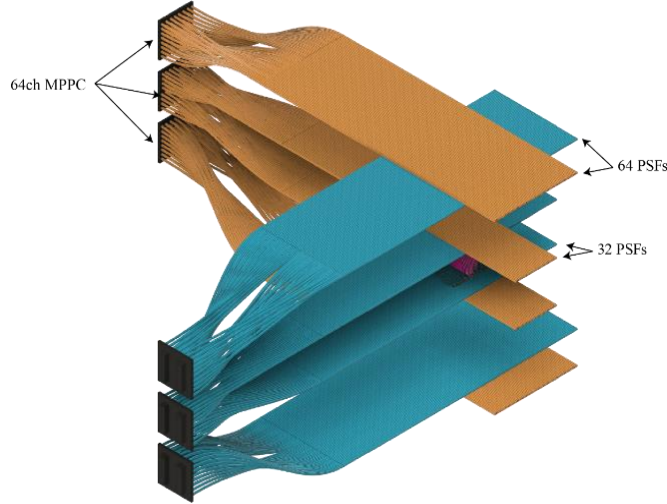


Fig. 1. Schematic view of  $\beta$ -NMR instrument

irradiating RF wave of NMR frequency. For example, two nuclear-spin-control techniques are frequently used. One is a depolarization method to erase polarization, and the other is an adiabatic-fast-passage method to flip the polarization. The nuclear spin of  $^{12}\text{B}$  causes

PSFs were connected to S13361-3050AE-08 multi-pixel photon counters (MPPCs) (Hamamatsu Photonics) [12] through  $\phi 2$ -mm optical fibers. The MPPC had 64 pixels. EASIROC modules [13] were used to control the MPPCs and read out signals from them. A



**Fig. 2.** Illustration of  $\beta$ -ray tracking detectors. Orange and blue detectors are mutually orthogonal

nuclei, electrons, and atoms of the sample elements to interact; therefore, their effects were observed as a shift in NMR frequencies and a decrease in polarization. Observing these phenomena made it possible to investigate inside the sample.

To add an imaging function,  $\beta$ -ray tracking detectors were constructed and installed in the  $\beta$ -NMR instrument, as shown in Fig. 2. The  $\beta$ -ray trackers consist of plastic scintillating fibers (PSFs) with cross sections of  $1\text{ mm} \times 1\text{ mm}$ . The PSF is SCSF-78 (Kuraray) [11]. Detector planes were constructed with 32 and 64 PSFs. The former and latter were placed near and far from the sample, respectively. The  $\beta$ -ray positions on the PSF plane were determined by the hit pattern of the PSFs. To determine the two-dimensional position, pairs of 32 and 64 PSF planes were installed in directions perpendicular to each other. The

VME-based data acquisition system [14] that consists of V1190A time-to-digital converters (CAEN) [15] was used for recording their signals. The  $\beta$ -ray hit positions on these planes were determined by PSFs, and the source positions of  $\beta$ -rays could be tracked back. Consequently, it was possible to reconstruct the source images.

Fig. 3 shows the full setup of the present  $\beta$ -MRI system viewed from the beam axis. Fig. 4 shows a photograph of its placement in the experimental hall of the HIMAC secondary beam course. To measure the total  $\beta$ -ray energy, the dipole-magnet poles have corn-shaped holes at their centers and large plastic scintillators placed at both outer ends. Because the  $\beta$ -ray energy distributes widely, measuring the total  $\beta$ -ray energy is essential for improving the imaging resolution.

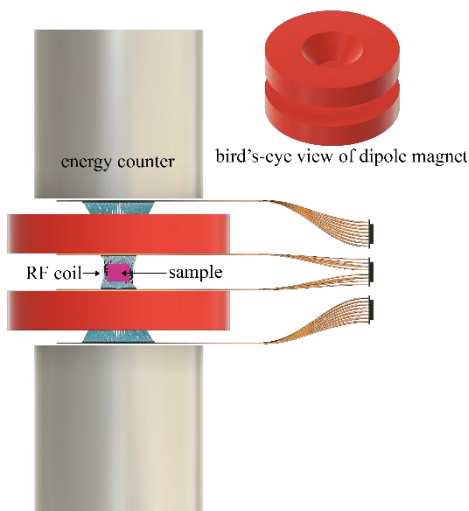


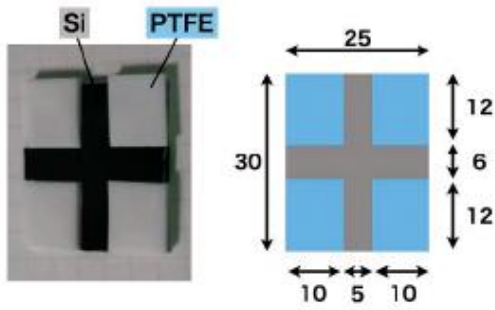
**Fig. 3.** Full setup of  $\beta$ -NMR system. Magnet poles have corn-shaped holes. Large plastic scintillators work as the energy counter



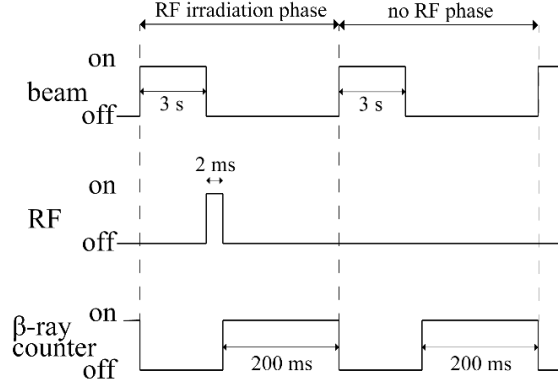
**Fig. 4.** Photograph of full setup of  $\beta$ -MRI system at HIMAC secondary beam course

Fig. 5 shows photograph of a sample consisting of cross-shaped silicon and four polytetrafluoroethylenes (PTFE) corners. Their sizes are also indicated in Fig. 5. This sample was installed at the center of the gap of the dipole magnet with a tilting angle of  $45^\circ$  with respect to the magnetic-field and

beam axes. Silicon has a diamond structure of a cubic crystalline nature, and the nuclear-spin polarization of  $^{12}\text{B}$  implanted in silicon is preserved [16]. However, polarization is not expected to be preserved inside polymers, such as PTFE. The asymmetry of the  $\beta$ -ray spatial distribution should be observed if  $\beta$ -



**Fig. 5.** Photograph of the sample (left side). Dimensions are indicated in millimeters (right side)



**Fig. 6.** Time sequence of beam, RF, and  $\beta$ -ray

rays are emitted from the silicon part of the sample, but the spatial asymmetry of the  $\beta$ -rays from the PTFE part will disappear. As a result, it should be possible to reconstruct the sample image by using the  $\beta$ -ray spatial asymmetry distribution, which depends on the  $\beta$ -ray source position.

To control the nuclear spin and observe NMR,  $^{12}\text{B}$  beams were irradiated with the time sequence shown in Fig. 6. The time sequence consists of two phases: one with RF irradiation and the other

without. Each phase has three parts: RI-beam irradiation, RF irradiation/no irradiation, and  $\beta$ -ray counting. By comparing the  $\beta$ -ray count rates of the upside and downside of each phase, one can estimate the polarization.

### III. RESULTS AND DISCUSSION

The experiment was performed for 15 h and  $5.6 \times 10^6$  events were accumulated. The data were analyzed, and preliminary results were obtained [17]. Because of accidental

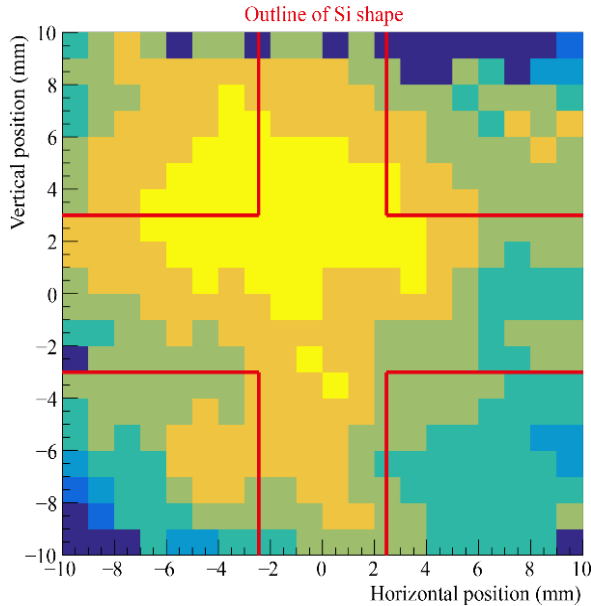


**Fig. 7.** Reconstructed image of the sample. Red line indicates Si shape

damage to the downside  $\beta$ -ray trackers, sufficient statistic could not be obtained. However, an attempted was made to evaluate the system. Fig. 7 shows a sample image reconstructed by  $\beta$ -ray tracking and  $\beta$ -NMR analysis. The relative intensity of  $\beta$ -ray spatial distribution's asymmetry is shown in a heatmap. Yellow indicates a large asymmetry, while blue indicates a small asymmetry. As the color transitions from blue to yellow, it indicates an increasing intensity of asymmetry. For the prediction, the polarization of  $^{12}\text{B}$  in the silicon part is preserved, while it disappears in the TPF part. Thus, a yellow pattern should appear with the shape of the silicon part. Fig. 7 shows the cross shape of the silicon part without sufficient resolution.

A computer simulation was performed using GEANT4 [18] to investigate the reason for the insufficient resolution. Because of the magnetic field, the  $\beta$ -ray, which consists of electrons, is affected by the Lorentz force. The present magnetic-field strength is 0.22 T. The magnetic field induced a degradation in the image resolution of 0.2 mm; therefore, it

was not the primary reason. Multiple scatterings of  $\beta$ -rays caused by the PSFs near the sample, which are 2-mm-thick plastics, induced a larger degradation. Figure 8 shows deviations in positions derived from the difference between the original and reconstructed positions of the  $\beta$ -rays. In the computer simulation,  $\beta$ -ray events were created that were emitted from the sample with random positions and energies. The  $\beta$ -rays passed through the PSFs, and the hit positions on the PSFs were recorded. After the simulation, the simulated  $\beta$ -ray tracks were analyzed, and the source position on the sample was reconstructed. The difference between the original and analyzed positions was calculated, as depicted in Fig. 8. If  $\beta$ -ray energy of more than 1 MeV is chosen, the deviation is 3.8 mm; if one of more than 10 MeV is chosen, the deviation is 1.5 mm; if one of more than 5 MeV is chosen, it is 1.5 mm. It was found that the image resolution depends primarily on the  $\beta$ -ray energy.

Fig. 9 shows the reconstructed sample image when a  $\beta$ -ray energy of more than 5 MeV is chosen. According to Fig.8, we expect that the resolution is 2.3 mm. The

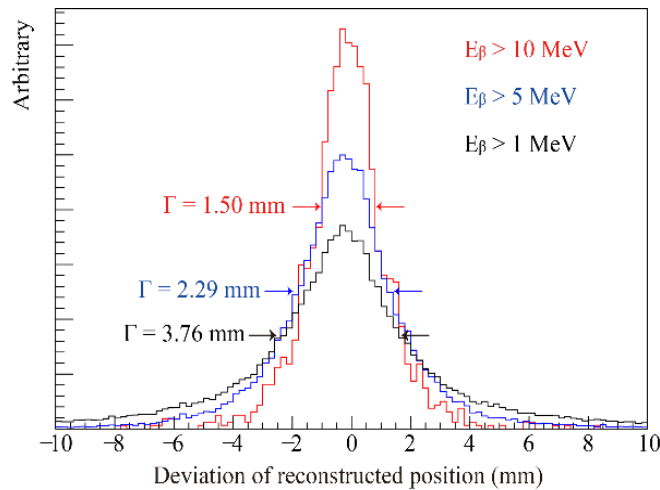


**Fig. 8** Deviation of reconstructed position.

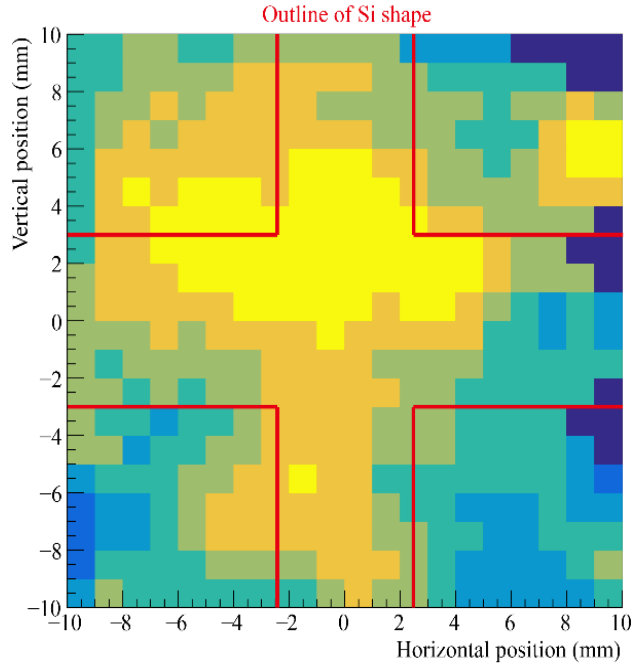


**Fig. 9** Reconstructed image obtained by choosing  $\beta$ -ray energy above 5 MeV.

image resolution is slightly improved compared with Fig. 7. It is better to increase the  $\beta$ -ray energy threshold to more than 10 MeV, but the events were insufficient to reproduce the image. Because the  $\beta$ -decay energy,  $Q$  value, of  $^{12}\text{B}$  is 13 MeV, the number of  $\beta$ -ray events above 10 MeV was small. To improve the image resolution, much-more-intense RI beams with higher  $Q$  values are required.

#### IV. CONCLUSION

A new MRI method,  $\beta$ -NMR, was constructed using the  $\beta$ -NMR technique. The  $\beta$ -MRI system was evaluated with nuclear-spin-polarized  $^{12}\text{B}$  beams and computer simulation. It was demonstrated that the  $\beta$ -MRI system works. The best image resolution achieved by the system was 2.3 mm. The image resolution was found to depend on the  $\beta$ -ray energies. This is important for improving the image

resolution. Applications of  $\beta$ -MRI should be investigated in future research.

#### ACKNOWLEDGEMENT

This work is supported by Fundamental Electronics Research Institute (FERI), Osaka Electro-Communication University (OECU).

#### REFERENCES

- [1]. I. I. Rabi, "Space Quantization in a Gyration Magnetic Field," *Phys. Rev.* 51, 652–654 (1937). DOI:10.1103/PhysRev.51.652.
- [2]. I. I. Rabi, J. R. Zacharias, S. Millman, P. Kusch, "A New Method of Measuring Nuclear Magnetic Moment," *Phys. Rev.* 53, 318 (1938). DOI:10.1103/PhysRev.53.318.
- [3]. T. Sugihara et al., "NMR Detection of Short-lived  $\beta$ -emitter  $^{12}\text{N}$  Implanted in Water," *Hyperfine Interact.* 20, 238–5 (2017). DOI:10.1007/s10751-017-1401-2.
- [4]. M. Mihara et al., "Beta-NMR of Short-lived Nucleus  $^{17}\text{N}$  in Liquids," *Hyperfine Interact.*

- 240, 113–9 (2019). DOI:10.1007/s10751-019-1650-3.
- [5]. P. C. Lauterbur, “Image Formation by Induced Local Interactions: Examples Employing Nuclear Magnetic Resonance,” *Nature* 242, 190–191 (1973). DOI:10.1038/242190a0.
- [6]. P. Mansfield, *NMR Imaging in Biomedicine* (Elsevier, 1982).
- [7]. Y. Mizoi et al., “Development of  $\beta$ -ray Tracker for  $\beta$ -NMR Spectroscopy and Imaging,” *Proc. of the 36<sup>th</sup> Workshop on Radiation Detectors and Their Uses, KEK Proc. 2022-3*, 54–63 (2023).
- [8]. K. Asahi et al., “New Aspect of Intermediate Energy Heavy Ion Reactions. Large Spin Polarization of Fragments,” *Phys. Lett. B* 251, 488–492 (1990). DOI:10.1016/0370-2693(90)90784-4.
- [9]. S. Kouda et al., “New Secondary Beam Course for Medical Use in HIMAC,” *1997 Particle Accelerator Conference, PAC’97 Proc.*, 3822–3824 (1997).
- [10]. M. Kanazawa et al., “Present Status of Secondary Beam Courses in HIHAC,” *Nucl. Phys. A* 746, 393c–396c (2004). DOI:10.1016/j.nuclphysa.2004.09.083.
- [11]. Kuraray Co. Ltd., <https://kuraray.com/>.
- [12]. Hamamatsu Photonics K. and K., <https://hamamatsu.com/>.
- [13]. I. Nakamura et al., “A 64ch readout module for PPD/MPPC/SiPM using EASIROC ASIC,” *Nucl. Instrum. Methods A* 787, 376–379 (2015). DOI: 10.1016/j.nima.2015.01.098.
- [14]. H. Baba et al., “MPV-Parallel Readout Architecture for the VME Data Acquisition System,” *IEEE Trans. Nucl. Sci.* 68, 1841–1848 (2021). DOI:10.1109/TNS.2021.3083832.
- [15]. CAEN S.p.A., <https://caen.it/>.
- [16]. T. Izumikawa, “[Hyperfine Interactions of Short-lived  $^{12}\text{B}$  in Si Crystal],” doctoral dissertation, Graduate School of Science, Osaka University, Japan, 1999.
- [17]. Y. Kimura, “[Development of Imaging Method using  $\beta$ -ray NMR],” master’s thesis, Graduate School of Science, Osaka University, Japan, 2023 [unpublished].
- [18]. S. Agostinelli et al., “Geant4 – a Simulation Toolkit,” *Nucl. Instrum. Methods Phys. Res. A* 506, 250–303 (2003). DOI:10.1016/S0168-9002(03)01368-8.